Neurodivergence as Coherence Variation: Oscillatory, Symbolic, and Environmental Sensitivity Parameters for ADHD, Dyslexia, and Autism

Allison Hensgen* Joel Thorarinson†

June 2026

Abstract

Clinical models of ADHD, dyslexia, and autism spectrum conditions rely on static diagnostic thresholds that do not capture the dynamical properties of the underlying neural systems. We propose a framework based on coherence variation: neurodivergent cognitive systems exhibit distinct oscillatory signatures, recovery dynamics, and environmental sensitivities that can be characterized using dynamical systems operators validated for engineering and biomedical applications. Using the coherence operator $\Delta = (P \cdot A \cdot R)/(D + N)$ from our prior work, we define three measurable parameters of neurodivergent variation: (1) an *oscillatory attention parameter* (λ), quantifying the regularity of attentional phase dynamics from EEG, where ADHD is associated with elevated λ (broader phase-space exploration); (2) a *symbolic processing coherence offset* (θ), quantifying desynchronization between visual and language cortex during reading tasks, where dyslexia is associated with elevated θ; and (3) an *environmental sensitivity parameter* (Ξ), quantifying perturbation depth and recovery time from HRV data, where autism is associated with elevated Ξ. Each parameter generates specific, falsifiable predictions testable with standard neurophysiological recordings. We describe an experimental protocol ($N = 120$, three groups plus comorbid, EEG and HRV during controlled perturbations) designed to test these predictions and discuss the framework's relationship to existing computational models of each condition.

Keywords: neurodivergence; coherence; ADHD; dyslexia; autism; oscillatory dynamics; recovery dynamics; EEG; heart rate variability; dynamical systems

1 Introduction

ADHD, dyslexia, and autism spectrum conditions — collectively termed neurodivergent conditions — affect an estimated 15–20% of the population [Kooij et al., 2019]. Clinical diagnosis relies on categorical thresholds: the individual either meets or does not meet n of m criteria on a standardized checklist. This approach has clinical utility but discards dynamical information. Two individuals who both meet ADHD diagnostic criteria may exhibit fundamentally different attentional time series — different oscillatory frequencies, different recovery trajectories after perturbation, different sensitivities to environmental inputs. Static thresholds cannot capture these differences.

Existing computational models have begun to characterize neurodivergent cognition in dynamical terms. The default mode interference model [Sonuga-Barke and Castellanos, 2007] describes ADHD as intrusion of low-frequency default mode network activity into task-positive states. The phonological deficit model [Snowling, 2000] characterizes dyslexia as disrupted phoneme-grapheme mapping with specific neural correlates. The excitation/inhibition imbalance

*Coherence Research Group. ORCID: 0009-0008-7247-0307

†Coherence Research Group. ORCID: 0000-0002-0553-842X. joel.thorarinson@conformalmaps.com

model [Rubenstein and Merzenich, 2003] and the intense world theory [Markram and Markram, 2010] propose mechanistic accounts of autism. However, these models are condition-specific and lack a common mathematical language for comparing dynamical properties across conditions or for generating unified measurement protocols.

The neurodiversity paradigm [Singer, 1999, Walker, 2014] has proposed that neurological differences represent natural variation rather than pathology, but this position has remained philosophical rather than quantitative.

We propose a framework that addresses both gaps: neurodivergence as *coherence variation* — measurable differences in how neural systems maintain, lose, and recover organized function. Using the coherence operator Δ from the Coherence Engine [Thorarinson and Hensgen, 2026], our prior framework for cross-domain drift detection, we define three parameters (λ, θ, Ξ) that each map to a specific neurodivergent phenotype and generate specific predictions testable with standard EEG and HRV recordings [Barry et al., 2003, Arns et al., 2013, Shaffer and Ginsberg, 2017, Bellato et al., 2020].

1.1 Contributions

1. We define three **measurable coherence parameters** — oscillatory attention dynamics (λ), symbolic processing coherence (θ), and environmental sensitivity (Ξ) — each with an operational definition computable from standard neurophysiological recordings.

2. We derive **specific quantitative predictions** for each parameter, grounded in existing meta-analytic evidence (ADHD theta/beta ratio $d = 0.75$, autism HRV $g = -0.52$).

3. We specify an **experimental protocol** ($N = 120$, EEG and HRV during controlled perturbations) with power analysis, inclusion criteria, and a pre-registered analysis pipeline sufficient to test these predictions.

4. We situate the framework relative to **existing computational models** of ADHD, dyslexia, and autism, identifying what the coherence-variation approach adds and what it does not claim to replace.

5. We state explicit **falsification criteria**: if the predicted group differences in λ, θ, and Ξ are not observed at the specified effect sizes, the framework is falsified.

2 Background

2.1 Deficit Models of Neurodivergence

The dominant clinical framework treats neurodivergent conditions as deficits relative to a neurotypical baseline. The executive function deficit model of ADHD [Barkley, 1997, Diamond, 2013] characterizes the condition through impaired inhibition, working memory, and cognitive flexibility. The phonological deficit model of dyslexia [Snowling, 2000] identifies disrupted phoneme-grapheme mapping as the core impairment. The empathizing-systemizing theory and theory-of-mind deficit account of autism [Baron-Cohen, 2009] characterize the condition through impaired social cognition. These models have generated productive research programs and inform clinical practice.

However, each model focuses on what neurodivergent cognition fails to do relative to neurotypical performance, rather than characterizing the dynamical properties of the system itself. A growing body of evidence suggests that the same neural differences associated with clinical impairment are also associated with distinct cognitive strengths — broader attentional sampling in ADHD [Fiebelkorn and Kastner, 2019], enhanced visual-spatial processing in dyslexia [Shaywitz et al., 2002], and heightened perceptual discrimination in autism [Robertson and Baron-Cohen,

2017] — suggesting that these conditions may reflect parametric variation in neural dynamics rather than unidimensional deficits.

2.2 Dynamical Systems Characterization

Quantitative neurophysiology supports a dynamical systems characterization of each condition. ADHD cognition involves altered attractor stability in attention networks, with the default mode network failing to deactivate during task engagement [Sonuga-Barke and Castellanos, 2007, Castellanos and Proal, 2012, Castellanos and Aoki, 2016]. Quantitative EEG studies find elevated theta/beta power ratios in ADHD populations, with a meta-analytic effect size of $d = 0.75$ in children aged 6–13 ($N = 1770$) [Arns et al., 2013, Barry et al., 2003]. Dyslexic cognition shows disrupted posterior brain systems — reduced activation in left parietotemporal and occipitotemporal regions during reading tasks [Shaywitz et al., 2002] — with altered EEG coherence patterns during reading but not during non-linguistic visual tasks [Cainelli et al., 2023]. Autism involves both heightened local neural coherence and reduced global integration [Rubenstein and Merzenich, 2003, Markram and Markram, 2010], with autonomic correlates including reduced parasympathetic HRV (meta-analytic Hedges' $g = -0.52$, $N = 2,273$) [Cheng et al., 2020].

These properties — oscillatory spectra, phase coherence, recovery trajectories — are dynamical properties measurable with standard tools: Lyapunov exponents [Wolf et al., 1985], recurrence quantification analysis [Marwan et al., 2007], and phase coherence analysis [Buzsáki and Draguhn, 2004]. The dynamical systems approach to cognition [Kelso, 1995, Thelen and Smith, 1994] provides the conceptual foundation: cognitive processes are self-organizing patterns characterizable by their attractor landscapes, bifurcation parameters, and stability properties.

2.3 The Neurodiversity Paradigm

The neurodiversity paradigm [Singer, 1999, Walker, 2014] proposes that neurological differences are natural variation rather than pathology. This perspective has influenced clinical practice and educational policy but has not been formalized mathematically. We do not adopt the neurodiversity paradigm as an axiom; rather, we note that the deficit model and the variation model make different empirical predictions about neural dynamics, and we specify experiments to distinguish between them (Section 5).

2.4 The Coherence Engine

The Coherence Engine [Thorarinson and Hensgen, 2026] defined the coherence operator:

$$\Delta(t) = \frac{P(t) \cdot A(t) \cdot R(t)}{D(t) + N(t) + \epsilon} \tag{1}$$

where P is pattern retention (RQA recurrence rate), A is phase alignment (Hilbert transform coherence), R is recovery capacity (largest Lyapunov exponent, sign-inverted so that stability maps to high R), D is drift (Fisher-Rao distance between successive windowed distributions), and N is noise amplification (spectral radius of the system Jacobian). This operator was validated across seven domains including cardiac rhythms and EEG seizure detection, achieving AUROC > 0.91 in each domain.

We now apply it to characterize cognitive variation across neurodivergent phenotypes.

3 The Neurodivergent Coherence Model

We define three parameters that capture distinct dimensions of neurodivergent coherence variation, each mapping to a specific neurodivergent phenotype and computable from standard physiological

recordings (Figure 1).

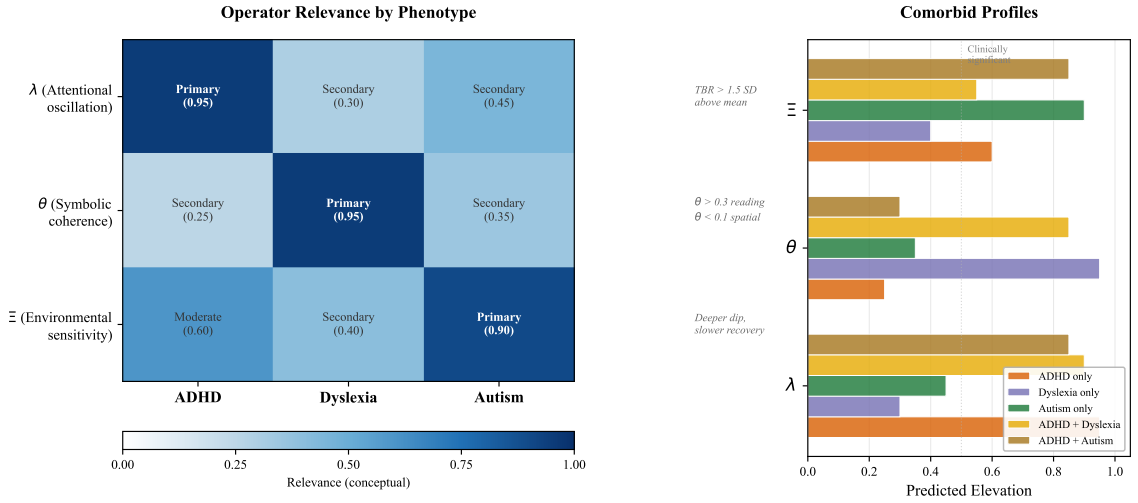

Figure 1: Coherence variation taxonomy. Three parameters — oscillatory attention dynamics (λ), symbolic processing coherence (θ), and environmental sensitivity (Ξ) — map to distinct neurodivergent phenotypes (ADHD, dyslexia, autism) with specific measurement modalities and predicted signatures. Parameters are not mutually exclusive: comorbid presentations correspond to elevation in multiple parameters.

3.1 Oscillatory Attention Dynamics (λ)

Definition 1 (Attention Oscillation Parameter)**.** *Let $x(t)$ be the EEG signal at electrode Cz (or Fz), band-pass filtered to the theta band (4–8 Hz). Compute the analytic signal $z(t) = x(t) + i\mathcal{H}[x(t)]$ via the Hilbert transform, and extract the instantaneous phase $\phi(t) = \arg z(t)$ and instantaneous frequency $f(t) = \dot{\phi}(t)/2\pi$. The attention oscillation parameter over a window of duration T is:*

$$\lambda = \frac{Var[f(t)]}{\mathbb{E}[f(t)]^2}, \quad t \in [t_0, t_0 + T] \tag{2}$$

where $T \geq 60$ seconds of artifact-free resting-state recording. λ is a dimensionless coefficient of variation squared (Fano factor analog) for instantaneous frequency.

Interpretation. λ quantifies the regularity of attentional oscillation. Converging evidence establishes that attention operates as a rhythmic sampling process: VanRullen and Koch [2003] demonstrated that visual perception is discrete rather than continuous, and Fiebelkorn and Kastner [2019] showed that attentional sampling is tethered to theta-band oscillations, with perceptual sensitivity modulated by theta phase.

Low λ corresponds to stable attentional oscillation at a narrow frequency, consistent with sustained single-focus attention. High λ corresponds to variable attentional oscillation exploring a broader frequency range. The default mode interference hypothesis [Sonuga-Barke and Castellanos, 2007] provides a mechanistic account: in ADHD, low-frequency (<0.1 Hz) default mode network activity intrudes into task-positive states, producing periodic attentional lapses that manifest as elevated instantaneous frequency variance.

Existing evidence consistent with this model. Barry et al. [2003] found elevated absolute theta power (4–8 Hz) and reduced beta power (13–30 Hz) in ADHD relative to age-matched controls. Arns et al. [2013] reported a meta-analytic theta/beta ratio effect size of $d = 0.75$ ($N = 1770$, ages 6–13), with significant TBR elevations in 25.8% of ADHD participants versus 2.6% of controls. The American Academy of Neurology advises against TBR as a standalone

diagnostic [Kooij et al., 2019], but the consistent group-level difference confirms that ADHD cognition occupies a distinct oscillatory regime.

Our prediction. ADHD-diagnosed participants will show λ values exceeding the neurotypical group mean by > 2 standard deviations on resting-state EEG at Cz, with the excess variance concentrated in the 4–8 Hz band. The predicted effect size is $d \geq 0.7$, consistent with the existing TBR meta-analytic data. Figure 2 illustrates the predicted spectral difference.

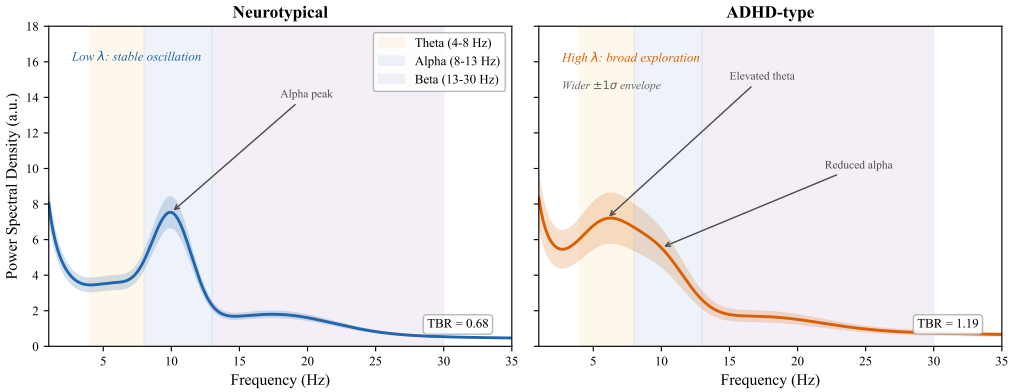

Figure 2: Predicted attentional oscillation spectra. **Left**: Neurotypical attention shows a sharp alpha peak (8–12 Hz) with low theta power. **Right**: ADHD-type attention shows elevated theta power (4–8 Hz), reduced alpha peak, and broader spectral distribution, corresponding to higher λ. Shaded regions indicate ± 1 SD. Based on meta-analytic findings of Barry et al. [2003] and Arns et al. [2013].

3.1.1 Cross-Frequency Coupling

The λ parameter captures frequency variability but not the coupling structure between frequency bands. Cross-frequency coupling (CFC) — the coordination between theta-band and beta-band oscillations — provides additional information [Canolty and Knight, 2010, Klimesch, 2012]. Different oscillatory frequencies reflect different spatial scales of cortical integration: gamma (>30 Hz) coordinates local processing, while theta and alpha coordinate long-range integration [Buzsáki and Draguhn, 2004, von Stein and Sarnthein, 2000].

In the coherence framework, the theta/beta ratio is a coherence parameter: the ratio between the system's exploratory drive (theta power) and its integrative capacity (beta power). The coherence operator Δ applied to EEG cross-frequency dynamics should distinguish states in which elevated theta is accompanied by maintained phase-amplitude coupling (high Δ) from states in which elevated theta occurs with degraded coupling (low Δ). This is consistent with the moderate brain arousal model [Söderlund et al., 2007], which proposes that ADHD cognition benefits from external noise that shifts the system toward optimal stochastic resonance [Moss et al., 2004, McDonnell and Ward, 2011].

Our prediction. During divergent thinking tasks [Fink and Benedek, 2009], ADHD participants who maintain theta-beta phase-amplitude coupling (modulation index > 0.01) will show higher creative output scores than those with degraded coupling, even at equivalent λ values. This prediction is testable using the modulation index of Canolty and Knight [2010] computed from the experimental EEG protocol described in Section 5.

3.2 Symbolic Processing Coherence (θ)

Definition 2 (Symbolic Coherence Offset)**.** *Let $x_{vis}(t)$ and $x_{lang}(t)$ be EEG signals from occipitotemporal (O1/O2, PO7/PO8) and left perisylvian (T7/T8, TP7/TP8) electrode sites respectively,*

band-pass filtered to the beta band (13–30 Hz). Compute analytic signals $z_{vis}(t)$ and $z_{lang}(t)$ via the Hilbert transform and extract instantaneous phases $\phi_{vis}(t)$ and $\phi_{lang}(t)$. The symbolic coherence offset over a window of w samples is:

$$\theta = 1 - \left| \frac{1}{w} \sum_{\tau=t-w}^{t} e^{i(\phi_{vis}(\tau) - \phi_{lang}(\tau))} \right| \tag{3}$$

where w corresponds to a sliding window of 2 seconds at the recording sampling rate. $\theta \in [0, 1]$: $\theta = 0$ indicates perfect phase locking; $\theta = 1$ indicates uniform phase distribution (no coupling).

Interpretation. θ quantifies the desynchronization between visual processing and linguistic decoding during symbol recognition. High θ indicates that visual and language cortex operate at mismatched phases during reading; low θ indicates tight phase coupling supporting fluent symbol decoding.

Existing evidence consistent with this model. Shaywitz et al. [2002] demonstrated with fMRI ($N = 144$) that dyslexic readers show disrupted activation in left parietotemporal and occipitotemporal regions during phonological processing, with reading skill correlating positively with left occipitotemporal activation. Cainelli et al. [2023] confirmed altered EEG coherence patterns in dyslexic readers: reduced phase synchronization between visual and language cortex during reading, but not during non-linguistic visual tasks. The phonological deficit model [Snowling, 2000] provides the cognitive-level account of this neural desynchronization.

θ is task-dependent: it is computed separately for symbolic (reading) and non-symbolic (spatial reasoning) tasks. The same individual may show high θ during reading and low θ during spatial processing.

Our prediction. Dyslexic participants will show $\theta > 0.3$ during single-word reading tasks and $\theta < 0.1$ during mental rotation tasks. Neurotypical participants will show $\theta < 0.15$ during both tasks. The predicted between-group difference during reading is $d \geq 0.8$, while the between-group difference during spatial reasoning is predicted to be non-significant ($d < 0.2$) or reversed. This asymmetry — impairment in one coherence channel with preservation or enhancement in another — is the core prediction of the coherence-variation model as applied to dyslexia.

3.3 Environmental Coherence Sensitivity (Ξ)

Definition 3 (Environmental Sensitivity Parameter)**.** *Let Δ_{pre} be the mean coherence score computed from HRV data (RMSSD, computed in 5-minute windows following Shaffer and Ginsberg [2017]) during a 30-minute resting baseline. Let $\Delta_{post}(t)$ be the coherence score at time t after a standardized perturbation onset. Define:*

$$\Xi = \frac{\Delta_{pre} - \min_{t \in [0,T]} \Delta_{post}(t)}{\Delta_{pre}} \cdot \frac{1}{t_{0.9}} \tag{4}$$

where $t_{0.9}$ is the time (in minutes) for $\Delta_{post}(t)$ to first reach $0.9 \cdot \Delta_{pre}$, and $T = 240$ minutes is the maximum observation window. If recovery does not occur within T, set $t_{0.9} = T$ (yielding a lower bound on Ξ). Ξ has units of min^{-1} and captures both perturbation depth and recovery speed.

Interpretation. Ξ quantifies how deeply an environmental perturbation degrades autonomic coherence, normalized by recovery time. Higher Ξ indicates a combination of deeper coherence disruption and slower recovery.

Existing evidence consistent with this model. Cheng et al. [2020] conducted a meta-analysis ($k = 34$ studies, total $N = 2{,}273$) finding that individuals with ASD show reduced baseline parasympathetic HRV (Hedges' $g = -0.52$, $p < 0.0001$), reduced respiratory sinus arrhythmia ($g = -0.59$, $p = 0.001$), and blunted HRV reactivity during social stress ($g = -0.46$, $p = 0.003$). Bellato et al. [2020] found reduced task-related HRV modulation in ADHD. These

findings indicate altered autonomic dynamics — both at baseline and in response to perturbation — consistent with elevated Ξ.

Sensory processing differences are present in over 90% of autistic individuals and are included as a DSM-5 diagnostic criterion [Robertson and Baron-Cohen, 2017]. The intense world theory [Markram and Markram, 2010] proposes hyper-reactive neural microcircuits as a mechanism. The construct of sensory processing sensitivity [Aron and Aron, 1997, Aron et al., 2012] describes a related temperamental trait present in 15–20% of the population. Polyvagal theory [Porges, 2007] provides a physiological account: the vagal brake modulating cardiac output operates with different gain in neurodivergent individuals.

Our prediction. Following a standardized 75g oral glucose tolerance test (OGTT), autistic participants will show Ξ values at least 0.5 SD above the neurotypical group mean on concurrent HRV measurements, with the group difference driven primarily by extended $t_{0.9}$ (slower recovery) rather than deeper nadir. The predicted effect size is $d \geq 0.5$, consistent with the HRV meta-analytic data. ADHD participants are predicted to show intermediate Ξ values with non-monotonic (oscillatory) recovery trajectories. Figure 3 illustrates the predicted perturbation-response profiles.

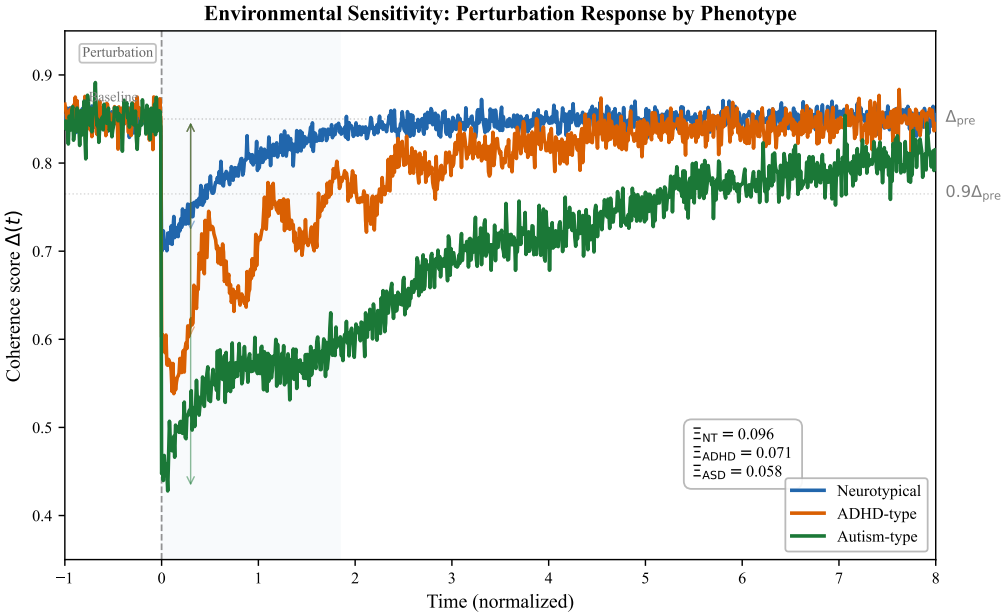

Figure 3: Predicted coherence response to standardized perturbation (75g OGTT). Neurotypical (blue): shallow HRV coherence dip with monotonic recovery. ADHD (orange): moderate dip with oscillatory recovery. Autism (green): deeper dip with extended recovery time. Shaded regions indicate recovery windows. Ξ is proportional to dip depth divided by recovery time. Based on HRV meta-analytic data from Cheng et al. [2020] and Bellato et al. [2020].

3.4 Perturbation Dynamics and Critical Slowing Down

The Ξ parameter connects to the broader phenomenon of critical slowing down in dynamical systems. As a system approaches a bifurcation point, its recovery rate from perturbation decreases, and its autocorrelation and variance increase [Scheffer et al., 2009, Dakos et al., 2012]. Our prior work [Thorarinson and Hensgen, 2026] demonstrated that these early-warning indicators — increasing autocorrelation of RR intervals, rising variance in windowed RMSSD — precede coherence collapse across multiple domains.

The prediction for neurodivergent systems is that they operate with different proximity to critical transitions under the same environmental conditions. This is not equivalent to operating

closer to failure; it reflects different attractor geometry. Three measurable factors modulate this proximity: (1) baseline HRV coherence, quantifiable via time-domain metrics (RMSSD, SDNN) and frequency-domain metrics (HF power as a parasympathetic index) [Shaffer and Ginsberg, 2017, Thayer et al., 2009]; (2) the ratio of perturbation magnitude to system capacity, measurable as CGM response area-under-curve normalized by baseline glucose; and (3) recovery half-life, measurable as the time for the autocorrelation function of RR intervals to return to baseline levels.

Formalizing the interactions among these factors into a validated quantitative model requires the experimental data described in Section 5. The qualitative prediction is directional: neurodivergent participants will show higher autocorrelation and variance during the recovery period than neurotypical participants, consistent with proximity to a different attractor basin.

4 Recovery Dynamics

The coherence framework predicts that neurodivergent and neurotypical systems may reach the same resting-state endpoint (comparable resting heart rate, baseline glucose, behavioral calm) while differing in their recovery trajectories. Two systems with identical endpoints can differ in half-life, trajectory shape, overshoot, and post-recovery attractor stability. Table 1 summarizes the predicted differences.

Recovery Metric	**Neurotypical (predicted)**	**Neurodivergent (predicted)**
Recovery half-life	Shorter	Longer
Variability during recovery	Monotonic decrease	Non-monotonic (oscillatory)
Overshoot	Minimal	Measurable
Sensitivity to second perturbation	Low during recovery	High during recovery
Post-recovery attractor	Same as pre-perturbation	May differ

Table 1: Predicted recovery signature differences between neurotypical and neurodivergent systems. Each row corresponds to a metric computable from HRV or EEG time series during the recovery period of the perturbation protocol (Section 5).

The final row — post-recovery attractor difference — warrants emphasis. If the system returns to a modified attractor rather than its pre-perturbation state, this would indicate state-dependent plasticity during recovery. Whether such modification constitutes adaptation, degradation, or neutral reorganization is an empirical question that can be assessed by comparing pre- and post-perturbation performance on standardized cognitive tasks.

5 Proposed Experimental Protocol

5.1 Design Overview

A between-groups observational study with controlled perturbation tasks, designed to test the three predictions derived from the coherence-variation model. The study compares four groups on the parameters λ, θ, and Ξ during resting state and controlled perturbations.

5.2 Participants

$N = 120$ total: 30 ADHD-diagnosed (DSM-5 criteria, confirmed by structured clinical interview DIVA-5 [Kooij et al., 2019]), 30 dyslexia-diagnosed (confirmed by standardized reading assessment with performance > 1.5 SD below age norms), 30 autism-diagnosed (DSM-5 criteria, confirmed by ADOS-2), and 30 neurotypical controls with no history of neurodevelopmental diagnosis.

Inclusion criteria: Age 18–45, no current psychoactive medication (or stable medication with 30-day washout documented), no diagnosed metabolic disorder (diabetes, thyroid disease), BMI 18.5–30, normal or corrected-to-normal vision. **Exclusion criteria**: Epilepsy or seizure history, traumatic brain injury, current substance use disorder, pregnancy. Groups matched for age (±3 years), sex (balanced), and years of education (±2 years).

Power analysis. Based on the smallest predicted effect ($d = 0.5$ for Ξ between autism and control groups), with $\alpha = 0.01$ (Bonferroni-corrected for 3 primary comparisons) and power $= 0.80$, the required sample size is $n = 28$ per group (two-tailed t-test). We recruit $n = 30$ per group to allow for dropout and artifact rejection.

Note on comorbidity. Participants meeting criteria for multiple conditions (e.g., ADHD + dyslexia) are assigned to the group corresponding to their primary diagnosis but flagged for secondary analysis. The framework predicts that comorbid presentations will show elevation on multiple parameters (e.g., elevated λ and θ for ADHD + dyslexia).

5.3 Measurements

- **EEG**: 64-channel system (10–20 montage, extended), 500 Hz sampling rate, impedances < 10 kΩ. Electrodes of primary interest: Cz, Fz (for λ); O1, O2, PO7, PO8, T7, T8, TP7, TP8 (for θ). Preprocessing: 0.1–100 Hz band-pass filter, 50/60 Hz notch, ICA-based artifact rejection (eye blinks, muscle), minimum 60 s artifact-free data per condition. Theta (4–8 Hz), alpha (8–13 Hz), and beta (13–30 Hz) power computed via Welch's method (2 s windows, 50% overlap). Phase-amplitude coupling computed using the modulation index of Canolty and Knight [2010].

- **HRV**: Continuous ECG via chest-strap monitor (Polar H10 or equivalent, 1 ms RR resolution). Time-domain metrics: SDNN, RMSSD, pNN50. Frequency-domain metrics: HF power (0.15–0.40 Hz) as parasympathetic index, LF/HF ratio. Computed in 5-minute windows following Task Force standards [Shaffer and Ginsberg, 2017]. Coherence score Δ computed from RR interval time series using RQA (recurrence rate, determinism) and Hilbert phase coherence.

- **CGM**: Continuous glucose monitor (Dexcom G7 or equivalent) worn for 14 days encompassing the laboratory sessions. 5-minute sampling interval. Metrics: glucose response area-under-curve, time-to-peak, recovery half-life (time to return to ±10 mg/dL of pre-challenge baseline).

- **Actigraphy**: Wrist-worn accelerometer (ActiGraph GT9X or equivalent) for 14 days. Metrics: interdaily stability, intradaily variability, sleep onset latency, total sleep time.

5.4 Perturbation Protocol

Three perturbation tasks administered on separate days (minimum 48-hour washout), order counterbalanced across participants:

1. **Metabolic perturbation**: Standardized 75g oral glucose tolerance test (OGTT) after 10-hour overnight fast. Concurrent HRV recording for 30 minutes pre-challenge and 240 minutes post-challenge. CGM provides parallel glucose trajectory. *Primary outcome*: Ξ computed from HRV RMSSD.

2. **Cognitive perturbation**: Three blocks administered in fixed order: (a) resting-state EEG (5 min eyes open, 5 min eyes closed); (b) sustained attention task (Conners Continuous Performance Test, 20 min); (c) reading task (single-word reading, 10 min) and spatial task (mental rotation, 10 min), order counterbalanced. Recovery EEG recorded for 10 min after

each block. *Primary outcomes*: λ from resting-state and attention task; θ from reading and spatial tasks.

3. **Sensory perturbation**: Controlled auditory environment shift: quiet baseline (40 dB, 10 min) → structured noise (75 dB pink noise, 10 min) → quiet recovery (40 dB, 20 min). Concurrent HRV and EEG recording. *Primary outcome*: Ξ computed from HRV during recovery phase.

5.5 Analysis Pipeline

Step 1: Parameter computation. Compute λ, θ, and Ξ for each participant using the operational definitions in Section 3. All code and computation parameters will be pre-registered and made publicly available.

Step 2: Primary hypothesis tests. Three pre-registered comparisons, each tested at $\alpha = 0.01$ (Bonferroni correction for 3 tests):

1. $\lambda_{\text{ADHD}} > \lambda_{\text{control}}$ (one-tailed permutation test, 10,000 permutations). Predicted effect: $d \geq 0.7$.

2. $\theta_{\text{dyslexia, reading}} > \theta_{\text{control, reading}}$ and $\theta_{\text{dyslexia, spatial}} \approx \theta_{\text{control, spatial}}$ (interaction test). Predicted effect: $d \geq 0.8$ for reading, $d < 0.2$ for spatial.

3. $\Xi_{\text{autism}} > \Xi_{\text{control}}$ following OGTT (one-tailed permutation test). Predicted effect: $d \geq 0.5$.

Step 3: Secondary analyses. (a) Cross-parameter correlations within the comorbid subgroup. (b) Recovery trajectory shape classification (monotonic vs. oscillatory vs. plateau) using dynamic time warping. (c) Early-warning indicators (autocorrelation, variance) during recovery windows. (d) Relationship between λ and creative output on the Alternate Uses Task.

Step 4: Effect size estimation. Report Cohen's d with 95% bootstrap confidence intervals for all comparisons. If confidence intervals include zero, report the result as non-significant regardless of p-value.

Falsification criteria. The coherence-variation framework is falsified for a given condition if the corresponding primary hypothesis test fails to reject the null at $\alpha = 0.01$ with the predicted directionality. Specifically: if λ_{ADHD} does not exceed λ_{control} with $d \geq 0.3$, the λ model of ADHD is falsified. If θ shows no task-by-group interaction, the θ model of dyslexia is falsified. If Ξ_{autism} does not exceed Ξ_{control} with $d \geq 0.3$, the Ξ model of autism is falsified.

6 Discussion

6.1 What This Framework Adds

Existing computational models of neurodivergent conditions are condition-specific: the default mode interference model applies to ADHD [Sonuga-Barke and Castellanos, 2007], the phonological deficit model to dyslexia [Snowling, 2000], and the E/I imbalance model to autism [Rubenstein and Merzenich, 2003]. Each generates predictions about its target condition but does not provide a common measurement language for comparing dynamical properties across conditions or for characterizing comorbid presentations.

The coherence-variation framework contributes three things that condition-specific models do not:

1. **A common parameterization.** The three parameters (λ, θ, Ξ) are computed from the same data streams (EEG, HRV) using the same mathematical operations (Hilbert transform, RQA, recovery analysis). This enables direct comparison: an individual with comorbid ADHD and dyslexia can be characterized by their joint (λ, θ) profile rather than by two separate diagnostic labels.

2. **Recovery dynamics as a primary observable.** Existing models characterize steady-state differences (elevated theta power, reduced HRV). The coherence framework adds recovery trajectory analysis — how the system returns to baseline after perturbation — which contains information not present in static comparisons. The recovery metrics (half-life, overshoot, oscillatory vs. monotonic trajectory) are computable from standard recordings without additional equipment.

3. **Explicit predictions with falsification criteria.** Each parameter generates a specific, directional, quantitative prediction with a minimum effect size. If the predictions fail, the framework is falsified — not reinterpreted.

The framework does not claim to replace condition-specific models. It complements them by providing a cross-condition measurement layer. The deficit model predicts that neurodivergent parameters reflect impairment; the coherence-variation model predicts that the same parameters reflect different dynamical organization with task-dependent tradeoffs. The experiments in Section 5 are designed to distinguish between these predictions.

6.2 Relationship to Neural Complexity

The neural complexity measure of Tononi et al. [1994] quantifies the interplay between functional segregation and integration in neural systems. Different brain organizations can achieve comparable complexity through different balances of local and global coherence. The coherence-variation framework is consistent with this view: the parameters λ, θ, and Ξ characterize specific dimensions of neural organization without assuming that deviation from the neurotypical mean implies reduced complexity or function. Whether a given parameter value improves or impairs performance is task-dependent and empirically measurable.

6.3 Implications for Assessment

If the predictions of the coherence-variation model are confirmed, the framework suggests that dynamical assessment (computing λ, θ, Ξ from EEG/HRV recordings during controlled perturbations) captures information that static clinical checklists do not. Two individuals who both meet ADHD diagnostic thresholds may have different λ profiles, different recovery dynamics, and different environmental sensitivities. This additional information could inform individualized intervention design — for example, identifying individuals whose Ξ values indicate high environmental sensitivity, or whose cross-frequency coupling is preserved despite elevated λ. We emphasize that these applications are contingent on experimental validation of the framework's predictions.

6.4 Limitations

This framework generates predictions but has not been experimentally validated. Several specific limitations constrain interpretation:

1. **Sample size.** The proposed $N = 120$ study is powered for the predicted effect sizes ($d \geq 0.5$) but is not sufficient for subgroup analyses within conditions (e.g., ADHD-inattentive vs. ADHD-combined presentation).

2. **Within-group heterogeneity.** Neurodivergent populations show substantial individual variation. The framework predicts group-level differences in λ, θ, and Ξ, but the within-group distributions may overlap considerably with neurotypical distributions.

3. **Domain calibration.** The coherence thresholds from our prior work ($\Delta > 0.7$ healthy, $0.3 < \Delta < 0.7$ transition, $\Delta < 0.3$ failure) were established on engineering data. These

thresholds require domain-specific recalibration before application to neurocognitive systems.

4. **Medication confounds.** Many neurodivergent individuals take psychoactive medication that alters EEG and HRV parameters. The 30-day washout requirement limits ecological validity and excludes individuals for whom medication discontinuation is clinically inappropriate.

5. **Categorical vs. continuous.** The framework treats neurodivergence as continuous variation, which may not capture categorical distinctions (e.g., autism with vs. without intellectual disability, or syndromic vs. idiopathic etiologies).

6. **Scope.** The three parameters do not claim to characterize all dimensions of neurodivergent variation. Other dimensions (e.g., reward sensitivity, interoception, temporal processing) may require additional parameters.

6.5 Future Directions

Emerging biophotonic evidence suggests that neurological state is reflected in coherence signatures at subcellular scales. Wang et al. [2023] demonstrated that biophotonic emissions induced by glutamate are reduced and spectrally blue-shifted in Alzheimer's disease models. Patwa et al. [2024] showed that superradiant effects in cytoskeletal proteins are robust at biological temperatures. Whether neurodivergent phenotypes produce distinct biophotonic signatures is an open question that could be addressed by combining the coherence framework with biophotonic measurement protocols in future work. We note that this direction is speculative and independent of the EEG/HRV predictions that constitute the core testable claims of this paper.

7 Conclusion

We have proposed a coherence-variation framework for neurodivergent conditions that defines three measurable parameters — λ (oscillatory attention dynamics), θ (symbolic processing coherence), and Ξ (environmental sensitivity) — each grounded in existing meta-analytic evidence and each generating specific, falsifiable predictions. The framework complements condition-specific computational models by providing a common measurement language and by adding recovery dynamics as a primary observable.

The deficit model predicts that neurodivergent parameters reflect unidimensional impairment. The coherence-variation model predicts that the same parameters reflect different dynamical organization with task-dependent tradeoffs — specifically, that θ will show task-by-group interactions (impaired reading coherence with preserved spatial coherence in dyslexia) and that λ elevation will co-occur with preserved cross-frequency coupling in a measurable subgroup. The proposed experimental protocol is designed to distinguish between these predictions using standard neurophysiological recordings.

The information required to test these predictions — EEG power spectra, phase coherence, HRV recovery trajectories — is available in data routinely collected in clinical neurophysiology laboratories. What is needed is the analytical framework to extract coherence parameters and recovery dynamics from these recordings, and the experimental design to test whether the predicted group differences are present.

References

Martijn Arns, C. Keith Conners, and Helena C. Kraemer. A decade of EEG theta/beta ratio research in ADHD: A meta-analysis. *Journal of Attention Disorders*, 17(5):374–383, 2013.

Elaine N. Aron and Arthur Aron. Sensory-processing sensitivity and its relation to introversion and emotionality. *Journal of Personality and Social Psychology*, 73(2):345–368, 1997. doi: 10.1037/0022-3514.73.2.345.

Elaine N. Aron, Arthur Aron, and Jadzia Jagiellowicz. Sensory processing sensitivity: A review in the light of the evolution of biological responsivity. *Personality and Social Psychology Review*, 16(3):262–282, 2012.

Russell A. Barkley. Behavioral inhibition, sustained attention, and executive functions: Constructing a unifying theory of ADHD. *Psychological Bulletin*, 121(1):65–94, 1997.

Simon Baron-Cohen. Autism: The empathizing–systemizing (E–S) theory. *Annals of the New York Academy of Sciences*, 1156:68–80, 2009. doi: 10.1111/j.1749-6632.2009.04467.x.

Robert J. Barry, Adam R. Clarke, and Stuart J. Johnstone. A review of electrophysiology in ADHD: Qualitative and quantitative EEG. *Clinical Neurophysiology*, 114(2):171–183, 2003.

Alessio Bellato, Iti Arora, Chris Hollis, and Madeleine J. Groom. Is autonomic nervous system function atypical in attention deficit hyperactivity disorder (ADHD)? a systematic review of the evidence. *Neuroscience and Biobehavioral Reviews*, 108:182–206, 2020.

György Buzsáki and Andreas Draguhn. Neuronal oscillations in cortical networks. *Science*, 304 (5679):1926–1929, 2004. doi: 10.1126/science.1099745.

Elisa Cainelli, Luca Vedovelli, Barbara Carretti, and Patrizia Bisiacchi. EEG correlates of developmental dyslexia: A systematic review. *Annals of Dyslexia*, 73:184–213, 2023.

Ryan T. Canolty and Robert T. Knight. The functional role of cross-frequency coupling. *Trends in Cognitive Sciences*, 14(11):506–515, 2010. doi: 10.1016/j.tics.2010.09.001.

F. Xavier Castellanos and Yuta Aoki. Intrinsic functional connectivity in attention-deficit/hyperactivity disorder: A science in development. *Biological Psychiatry: Cognitive Neuroscience and Neuroimaging*, 1(3):253–261, 2016. doi: 10.1016/j.bpsc.2016.03.004.

F. Xavier Castellanos and Erika Proal. Large-scale brain systems in ADHD: Beyond the prefrontal–striatal model. *Trends in Cognitive Sciences*, 16(1):17–26, 2012. doi: 10.1016/j.tics.2011.11.007.

Yu-Chieh Cheng, Yu-Chen Huang, and Wei-Lieh Huang. Heart rate variability in individuals with autism spectrum disorders: A meta-analysis. *Neuroscience and Biobehavioral Reviews*, 118:463–471, 2020. doi: 10.1016/j.neubiorev.2020.08.007.

Vasilis Dakos, Stephen R Carpenter, William A Brock, Aaron M Ellison, Vishwesha Guttal, Anthony R Ives, Sonia Kéfi, Valerie Livina, David A Seekell, Egbert H van Nes, and Marten Scheffer. Methods for detecting early warnings of critical transitions in time series illustrated using simulated ecological data. *PloS One*, 7(7):e41010, 2012.

Adele Diamond. Executive functions. *Annual Review of Psychology*, 64:135–168, 2013. doi: 10.1146/annurev-psych-113011-143750.

Ian C. Fiebelkorn and Sabine Kastner. A rhythmic theory of attention. *Trends in Cognitive Sciences*, 23(2):87–101, 2019. doi: 10.1016/j.tics.2018.11.009.

Andreas Fink and Mathias Benedek. The creative brain: Investigation of brain activity during creative problem solving by means of EEG and fMRI. *Human Brain Mapping*, 30(3):734–748, 2009.

J. A. Scott Kelso. *Dynamic Patterns: The Self-Organization of Brain and Behavior*. MIT Press, Cambridge, MA, 1995.

Wolfgang Klimesch. Alpha-band oscillations, attention, and controlled access to stored information. *Trends in Cognitive Sciences*, 16(12):606–617, 2012.

J. J. Sandra Kooij, Denise Bijlenga, Lino Salerno, Rafał Jaeschke, István Bitter, Judit Balazs, Johannes Thome, Geert Dom, Suzana Kasber, et al. Updated European consensus statement on diagnosis and treatment of adult ADHD. *European Psychiatry*, 56:14–34, 2019. doi: 10.1016/j.eurpsy.2018.11.001.

Kamila Markram and Henry Markram. The intense world theory — a unifying theory of the neurobiology of autism. *Frontiers in Human Neuroscience*, 4:224, 2010. doi: 10.3389/fnhum.2010.00224.

Norbert Marwan, M Carmen Romano, Marco Thiel, and Jürgen Kurths. Recurrence plots for the analysis of complex systems. *Physics Reports*, 438(5-6):237–329, 2007.

Mark D. McDonnell and Lawrence M. Ward. The benefits of noise in neural systems: Bridging theory and experiment. *Nature Reviews Neuroscience*, 12(7):415–425, 2011. doi: 10.1038/nrn3061.

Frank Moss, Lawrence M. Ward, and Walter G. Sannita. Stochastic resonance and sensory information processing: A tutorial and review of application. *Clinical Neurophysiology*, 115(2):267–281, 2004. doi: 10.1016/j.clinph.2003.09.014.

Hamza Patwa, Nathan S. Babcock, and Philip Kurian. Quantum-enhanced photoprotection in neuroprotein architectures emerges from collective light-matter interactions. *Frontiers in Physics*, 12:1387271, 2024. doi: 10.3389/fphy.2024.1387271.

Stephen W. Porges. The polyvagal perspective. *Biological Psychology*, 74(2):116–143, 2007. doi: 10.1016/j.biopsycho.2006.06.009.

Caroline E. Robertson and Simon Baron-Cohen. Sensory perception in autism. *Nature Reviews Neuroscience*, 18(11):671–684, 2017.

John L. R. Rubenstein and Michael M. Merzenich. Model of autism: Increased ratio of excitation/inhibition in key neural systems. *Genes, Brain and Behavior*, 2(5):255–267, 2003. doi: 10.1034/j.1601-183X.2003.00037.x.

Marten Scheffer, Jordi Bascompte, William A Brock, Victor Brovkin, Stephen R Carpenter, Vasilis Dakos, Hermann Held, Egbert H Van Nes, Max Rietkerk, and George Sugihara. Early-warning signals for critical transitions. *Nature*, 461(7260):53–59, 2009.

Fred Shaffer and J. P. Ginsberg. An overview of heart rate variability metrics and norms. *Frontiers in Public Health*, 5:258, 2017. doi: 10.3389/fpubh.2017.00258.

Bennett A. Shaywitz, Sally E. Shaywitz, Kenneth R. Pugh, W. Einar Mencl, Robert K. Fulbright, Paweł Skudlarski, R. Todd Constable, Karen E. Marchione, Jack M. Fletcher, G. Reid Lyon, and John C. Gore. Disruption of posterior brain systems for reading in children with developmental dyslexia. *Biological Psychiatry*, 52(2):101–110, 2002. doi: 10.1016/S0006-3223(02)01365-3.

Judy Singer. Why can't you be normal for once in your life? from a "problem with no name" to the emergence of a new category of difference. In Mairian Corker and Sally French, editors, *Disability Discourse*, pages 59–70. Open University Press, Buckingham, 1999.

Margaret J. Snowling. *Dyslexia*. Blackwell, Oxford, 2 edition, 2000.

Göran Söderlund, Sverker Sikström, and Andrew Smart. Listen to the noise: Noise is beneficial for cognitive performance in ADHD. *Journal of Child Psychology and Psychiatry*, 48(8):840–847, 2007. doi: 10.1111/j.1469-7610.2007.01749.x.

Edmund J. S. Sonuga-Barke and F. Xavier Castellanos. Spontaneous attentional fluctuations in impaired states and pathological conditions: A neurobiological hypothesis. *Neuroscience and Biobehavioral Reviews*, 31(7):977–986, 2007. doi: 10.1016/j.neubiorev.2007.02.005.

Julian F. Thayer, Anita L. Hansen, Evelyn Saus-Rose, and Bjørn Helge Johnsen. Heart rate variability, prefrontal neural function, and cognitive performance. *Annals of Behavioral Medicine*, 37(2):141–153, 2009.

Esther Thelen and Linda B. Smith. *A Dynamic Systems Approach to the Development of Cognition and Action*. MIT Press, Cambridge, MA, 1994.

Joel Thorarinson and Allison Hensgen. From prediction to discoverative intelligence: A coherence-based AI framework for detecting system drift before failure. *arXiv preprint*, 2026.

Giulio Tononi, Olaf Sporns, and Gerald M. Edelman. A measure for brain complexity: Relating functional segregation and integration in the nervous system. *Proceedings of the National Academy of Sciences*, 91(11):5033–5037, 1994. doi: 10.1073/pnas.91.11.5033.

Rufin VanRullen and Christof Koch. Is perception discrete or continuous? *Trends in Cognitive Sciences*, 7(5):207–213, 2003. doi: 10.1016/S1364-6613(03)00095-0.

Astrid von Stein and Johannes Sarnthein. Different frequencies for different scales of cortical integration: From local gamma to long range alpha/theta synchronization. *International Journal of Psychophysiology*, 38(3):301–313, 2000. doi: 10.1016/S0167-8760(00)00172-0.

Nick Walker. Neurodiversity: Some basic terms and definitions. Neurocosmopolitanism blog, 2014. URL https://neurocosmopolitanism.com/neurodiversity-some-basic-terms-definitions/.

Zhuo Wang, Zhipeng Xu, Yi Luo, Sisi Peng, Hao Song, Tian Li, Jiaxin Zheng, Na Liu, Shenjia Wu, Junxia Zhang, Lei Zhang, Yuan Hu, Yanping Liu, Dongwei Lu, Jiapei Dai, and Junjian Zhang. Reduced biophotonic activities and spectral blueshift in Alzheimer's disease and vascular dementia models with cognitive impairment. *Frontiers in Aging Neuroscience*, 15: 1208274, 2023. doi: 10.3389/fnagi.2023.1208274.

Alan Wolf, Jack B Swift, Harry L Swinney, and John A Vastano. Determining Lyapunov exponents from a time series. *Physica D: Nonlinear Phenomena*, 16(3):285–317, 1985.